Terahertz Attenuation and Dispersion Characteristics of Coplanar Transmission Lines

Michael Y. Frankel, *Student Member, IEEE*, Shantanu Gupta, Janis A. Valdmanis, and Gerard A. Mourou, *Member, IEEE*

Abstract—**We present experimental verification of analytic formulas for the dispersion and the attenuation of electrical transient signals propagating on coplanar transmission lines. The verification is done in the frequency domain over a teraherz range, although the experiments are in the time domain. The analytic formulas have been obtained from fits to the full-wave analysis results. We quantitatively verify that the full-wave steady-state solutions can be directly applied to the transient time-domain propagation experiments. We use subpicosecond electrical pulses and an external electro-optic sampling technique to obtain the time-domain propagation data. From the Fourier transforms of the time-domain data we extract both the attenuation and the phase information as a function of frequency. The dispersion and the attenuation characteristics are investigated for both coplanar waveguide and coplanar strip transmission lines. The investigation was also carried out on both semi-insulating semiconductor and dielectric substrate materials and indicates no observable losses caused by the semiconductor material.**

I. Introduction

THE recent progress in semiconductor devices has advanced their response frequencies above 400 GHz [1]. Such bandwidths well exceed the range of validity of the quasi-static approximations that are often made in modeling the propagation of the electrical signals on transmission line interconnects. Also, the measurements of the transmission line propagation properties have been applied to more fundamental studies such as the extraction of material parameters for high-temperature superconducting films in the subterahertz frequency region [2], [3]. The requirement for transmission line interconnect modeling as well as the application of the propagation measurements to material characterization necessitates a precise knowledge of the transmission line dispersion and attenuation characteristics. It is also of tremendous practical benefit to allow such computations to be carried out analytically.

Manuscript received August 27, 1990; revised January 17, 1991. This work was supported by the Air Force Office of Scientific Research, University Research Initiative, under Contract F49620-87-C-0016.

The authors are with the Department of Electrical Engineering and Computer Science, University of Michigan, Ann Arbor, MI 48109-2099.

IEEE Log Number 9144292.

Hasnain *et al.* [4] have proposed an analytic formula, fitted to full-wave analysis results, to model the dispersion characteristics of coplanar transmission lines (CTL's) in the frequency domain. They have qualitatively shown the formula's applicability in modeling time-domain pulse propagation. However, the experimental signal bandwidth was limited to below 200 GHz, and no quantitative frequency-domain comparisons were performed.

In addition to the dispersion characteristics, the attenuation becomes important at high frequencies. Grischkowsky *et al.* [5] have experimentally demonstrated that the radiative losses are dominant for frequencies over ~ 200 GHz for CTL dimensions of the order of a few tens of microns. Rutledge *et al.* [6] have derived analytic formulas to model the radiative attenuation of CTL's in the frequency domain under quasi-static approximations. However, the measured attention was a factor of 1.5 higher than the one computed from the analytic formula. In addition, the functional frequency dependence of the measured attenuation deviated from that predicted by the formula. More recently, Phatak *et al.* [7] have proposed modifications to the analytic attenuation formulas for coplanar strip transmission lines and have compared them with full-wave analysis results. The experimental validation was done qualitatively in the time domain only.

It is reasonable to question the applicability of the dispersion and attenuation formulas obtained from fitting the full-wave analysis results to time-domain propagation modeling. The approach that is used in full-wave analysis assumes a continuous wave (CW) type of excitation of a transmission line, and the substrate thickness is explicitly included in the analysis and the approximations. However, the time-domain propagation data are obtained from an inherently transient experiment. The signal round-trip time across typical 500-μm-thick substrates exceeds the measurement time windows used for picosecond transient measurements. To the best of the authors' knowledge, no quantitative comparisons have been performed between the measurements and the analytic formulas in the fre-

0018-9480/91/0600-0910$01.00

quency domain to THz frequencies. Thus, a direct frequency-domain comparison is desirable to show that the frequency-domain full-wave solutions apply to the time-domain transient propagation experiments.

In this paper we experimentally demonstrate the applicability of the semiempirical analytic dispersion formula to the modeling of the subpicosecond electrical pulse propagation on CTL's. We also show the significant inaccuracy in making quasi-static approximations in modeling the electrical signal attenuation behavior at frequencies in the hundreds of gigaherz. We present modified analytic formulas and experimentally demonstrate their validity to THz frequencies. Both the dispersion and the attenuation comparisons are carried out quantitatively in the frequency domain.

The dispersion and the attenuation characteristics are expressed analytically allowing for a convenient and efficient CTL design procedure. For maximum generality, the experimental measurements are carried out on both semi-insulating semiconductor and dielectric substrates with both coplanar waveguide (CPW) and coplanar strip (CPS) transmission lines.

II. Theory

We select CTL's for the present investigation. They offer an advantage over more conventional microstrip lines in that their dimensions, and therefore their propagation properties, are defined by the lithographic limits. Also, CTL's have recently been applied as signal feed lines to a transistor for small-signal parameter extraction at frequencies up to 100 GHz [8]. Similar lines have been used for investigating the intrinsic material properties of high-temperature superconductors [3].

Electrical signal propagation is conventionally modeled in the frequency domain. Thus, the signal propagation on transmission lines is assumed to be described in phasor notation as

$$V(f,z) = V(f,0)e^{-(\alpha(f)+j\beta(f))z} \tag{1}$$

where $V(f,z)$ is the Fourier transform of the time-domain waveform at a distance z, $\alpha(f)$ is the frequency-dependent attenuation, and $\beta(f)$ is the frequency-dependent phase.

A. Dispersion Characteristics

The dispersive characteristics of coplanar transmission lines have been modeled numerically and analytically by Hasnain *et al.* [4]. In that work, an analytic approximation has been derived from a numerical simulation. The phase is modeled as

$$\beta(f) = 2\pi\frac{f}{c}\sqrt{\epsilon_{\text{eff}}(f)} \tag{2}$$

where $\epsilon_{\text{eff}}(f)$ is the effective dielectric constant, analytically approximated by

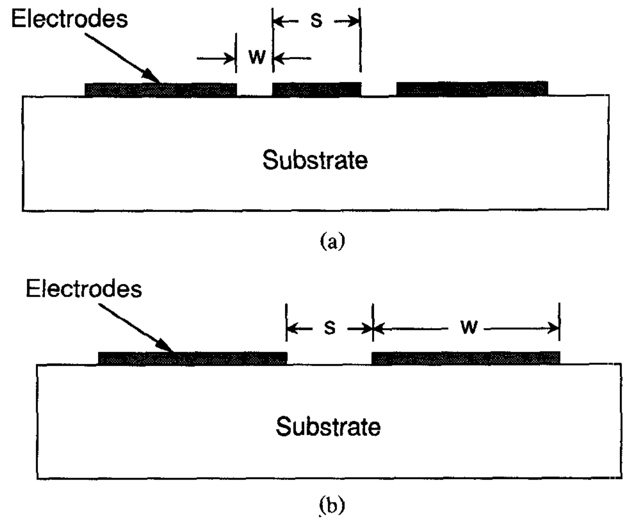

Fig. 1. Cross-sectional view of the investigated transmission lines. (a) Coplanar waveguide (CPW). (b) Coplanar strip (CPS).

$$\sqrt{\epsilon_{\text{eff}}(f)} = \sqrt{\epsilon_q} + \frac{\left(\sqrt{\epsilon_r} - \sqrt{\epsilon_q}\right)}{\left(1 + a\left(\dfrac{f}{f_{\text{te}}}\right)^{-b}\right)}. \tag{3}$$

Here

$$\epsilon_q = \frac{\epsilon_r + 1}{2}$$

is the quasi-static effective permittivity,

$$f_{\text{te}} = \frac{c}{4d\sqrt{\epsilon_r - 1}} \tag{4a}$$

is the surface wave TE_1 mode cutoff frequency, b (~ 1.8) is taken to be independent of geometry, ϵ_r is the relative permittivity of the substrate material, and c is the speed of light in vacuum. The parameter a is related to the transmission line geometry as

$$\log(a) \sim u \log(s/w) + v \tag{4b}$$

where

$$u \sim 0.54 - 0.64q + 0.015q^2$$
$$v \sim 0.43 - 0.86q + 0.54q^2$$
$$q = \log(s/d).$$

For the CPW and CPS lines the geometric parameters s, w, and d are as shown in parts (a) and (b) of Fig. 1. It is important to note that (3) is semiempirical and makes no quasi-static assumptions.

B. Attenuation Characteristics

As was pointed out in the introduction, the attenuation is expected to be dominated by the radiative losses for frequencies over 200 GHz [5]. It has been shown by Rutledge *et al.* [6] that the attenuation should follow a cubic frequency dependence under quasi-static approximations. For example, for a CPW, the attenuation is given as

$$\alpha=\left(\frac{\pi}{2}\right)^{5}\frac{1}{\sqrt{2}}\frac{(1-1/\epsilon_r)^2}{\sqrt{1+1/\epsilon_r}}\frac{(s+2w)^2\epsilon_r^{3/2}}{c^3K'(k)K(k)}f^3 \quad (5)$$

where the frequency dependence arises explicitly from the f^3 term. In (5), $k=s/(s+2w)$, $K(k)$ is the complete elliptic integral of the first kind, and $K'(k)=K(\sqrt{1-k^2})$.

Our experimental data, which are discussed in Section IV, indicate that this formula is not valid near THz frequencies. Plotting the frequency dependence of the measured attenuation on a log–log scale shows that the slope is significantly below 3, the behavior predicted by (5). We believe that this discrepancy is due to significant inaccuracies introduced by the quasi-static approximation at high frequencies. In this work, we follow the derivation of the radiative attenuation as outlined in [6] but also analytically include the non-quasi-static effects as discussed below. This approach is similar to the one used by Phatak *et al.* [7].

The propagating guided signal mode travels with a velocity which is faster that the electromagnetic propagation velocity in the substrate. Thus, the guided mode loses energy through an electromagnetic shock wave which is emitted into the substrate at a radiation angle Ψ. Rutledge *et al.* [6] have shown that the magnitude of the attenuation depends critically on this angle. The angle Ψ is determined by the velocity mismatch between the guided and the radiated modes as

$$\cos(\Psi)=\frac{k_z}{k_d} \quad (6)$$

where k_z and k_d are the guided and dielectric substrate propagation constants respectively. This quantity can also be rewritten in terms of the permittivities as

$$\cos(\Psi)=\frac{\sqrt{\epsilon_{\text{eff}}(f)}}{\sqrt{\epsilon_r}} \quad (7)$$

where ϵ_{eff} is the effective permittivity experienced by the guided mode and ϵ_r is the dielectric substrate permittivity experienced by the shock wave.

We assume that the effective permittivity obtained from the dispersion analysis and (3) applies to the calculation of the attenuation as well. This assumption is justified since both effective permittivities describe the guided mode phase velocity characteristics. The higher guided mode frequencies are more confined to the substrate, leading to an increase in k_z with a corresponding increase in ϵ_{eff} and the commonly observed electrical signal dispersion. The radiation angle becomes frequency dependent, modifying the frequency dependence of the attenuation. We also point out that as ϵ_{eff} approaches ϵ_r at very high frequencies, the radiative angle, Ψ, approaches 0, eliminating the shock wave radiation. Similarly, we use the ϵ_{eff} from (3) to account for the characteristic impedance variation with frequency as

$$Z_{\text{cpw}}=\frac{120\pi}{\sqrt{\epsilon_{\text{eff}}(f)}}\frac{K'(k)}{4K(k)},\quad \text{for a coplanar waveguide} \quad (8a)$$

$$Z_{\text{cps}}=\frac{120\pi}{\sqrt{\epsilon_{\text{eff}}(f)}}\frac{K(k)}{K'(k)},\quad \text{for a coplanar stripline.} \quad (8b)$$

Furthermore, we correct a prefactor error in the CPS attenuation coefficient formula.

As will be shown in the discussion of the experimental measurements in Section IV, these modifications result in excellent agreement between the functional frequency dependence of the measured and computed attenuation to THz frequencies. The experimental attenuation is further supported by the fully numeric time-domain transmission line matrix method simulations [9].

With the above frequency-dependent corrections applied to the radiation angle, Ψ, and the characteristic impedance, Z_0, the radiative attenuation coefficients become, for a CPW,

$$\alpha_{\text{cpw}}=\left(\frac{\pi}{2}\right)^{5}2\left(\frac{\left(1-\frac{\epsilon_{\text{eff}}(f)}{\epsilon_r}\right)^2}{\sqrt{\frac{\epsilon_{\text{eff}}(f)}{\epsilon_r}}}\right)\frac{(s+2w)^2\epsilon_r^{3/2}}{c^3K'(k)K(k)}f^3 \quad (9a)$$

and for a CPS

$$\alpha_{\text{cps}}=\pi^5\frac{(3-\sqrt{8})}{2}\sqrt{\frac{\epsilon_{\text{eff}}(f)}{\epsilon_r}}\cdot\left(1-\frac{\epsilon_{\text{eff}}(f)}{\epsilon_r}\right)^2\frac{(s+2w)^2\epsilon_r^{3/2}}{c^3K'(k)K(k)}f^3. \quad (9b)$$

These equations are expected to be valid for geometries approximately constrained by $0.1<s/w<10$ and $d>3w$ and for wavelengths $\lambda>s+2w$.

To appreciate the influence of the non-quasi-static effects on the results, we plot in Fig. 2 the radiative attenuation computed from (9a) for several CPW transmission line geometries on GaAs substrate. For comparison, we also include the results from a quasi-static equation, (5), for one of the geometries as curve (*iii*). Even for small geometries, the attenuation shown by curves (*i*) and (*ii*) exhibits an appreciable deviation from a simple cubic frequency dependence. With increasing CPW dimensions, the low-frequency attenuation increases as $(s+2w)^2$, as evidenced by curves (*i*), (*iv*), and (*v*). However, the high-frequency roll-off is also stronger, leading to an overall smaller attenuation at the highest frequencies. This result may be of practical significance in transmission line design.

The surface wave attenuation is not important for the present investigation because the substrate thickness is much greater than the CTL dimensions, and the signal round-trip time across the substrate is greater than the

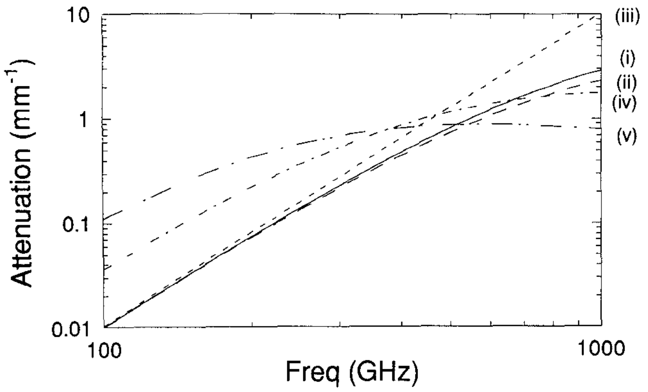

Fig. 2. Radiative attenuation computed from eq. (9a) on a log–log scale. (*i*) $s = 30$ μm, $w = 20$ μm, $d = 500$ μm, $a = 334$, $f_{te} = 43$ GHz; (*ii*) $s = 30$ μm, $w = 20$ μm, $d = 250$ μm, $a = 86$, $f_{te} = 76$ GHz; (*iii*) Quasi-static approximation for same dimensions as (*i*) with $a \to \infty$; (*iv*) $s = 60$ μm, $w = 40$ μm, $d = 500$ μm, $a = 76$, $f_{te} = 43$ GHz; (*v*) $s = 120$ μm, $w = 180$ μm, $d = 500$ μm, $a = 21$, $f_{te} = 43$ GHz.

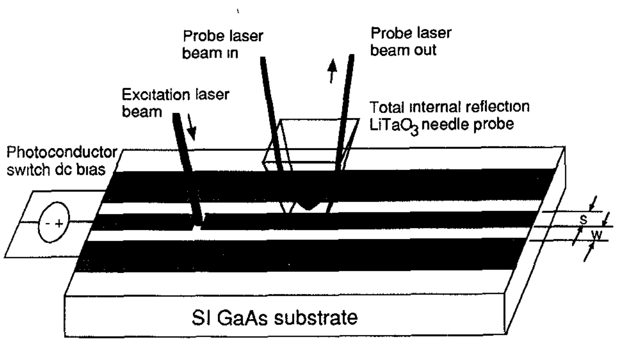

Fig. 3. Typical excitation and electro-optic sampling geometry for a coplanar waveguide.

measurement time window. Therefore, the attenuation should be dominated by the radiative term only.

An additional attenuation term can be added to account for the conductor skin-effect losses. These losses are assumed to obey the conventionally accepted behavior and follow a square root frequency dependence [10]. They are almost negligible compared with the radiative attenuation for frequencies above 200 GHz, but are still taken into account. The dielectric losses, to a good approximation, can be ignored for the substrate materials investigated.

III. Experiment

The experimental data are presented for a CPS fabricated on a 430-μm-thick sapphire substrate and for a CPW fabricated on a 500-μm-thick GaAs substrate using standard photolithographic techniques. The conducting electrode was 0.4 μm of Al metal for the CPS and 0.05/0.35 μm of Ti/Au metal for the CPW.

In these experiments the THz bandwidth, subpicosecond electrical pulses are produced by a gap photoconductor switch [11]. As shown in Fig. 3, a gap between the conductors in a CTL behaves as an open circuit until it is illuminated by the 100 fs laser pulses from a balanced colliding-pulse mode-locked (CPM) dye laser [12]. The photogenerated carriers increase the switch conductivity. The dc electric field applied across the switch is disturbed, causing a voltage transient to be launched onto the CTL. The transient duration is determined primarily by the carrier lifetime in the photoconductor material. The CPS uses ion-implant damaged silicon-on-sapphire (SOS) as the photoconducting material. To eliminate any possible influence of the semiconductor film on the CPS measurements, the silicon is etched off everywhere except for a small patch which defines the switch. The CPW uses low-temperature molecular beam epitaxial grown GaAs (LT-GaAs) material. The SOS and the LT-GaAs materials have subpicosecond carrier lifetimes [13], resulting in subpicosecond fall times of the electrical pulses. Typical full width at half maximum (FWHM) for the generated electrical pulses is ~ 0.6 ps; therefore, they have a 3 dB bandwidth of ~ 500 GHz.

External electro-optic sampling techniques with a $LiTaO_3$ probe tip are used to measure the picosecond electrical transients [14]. The probe has a 40×40 μm^2 face and can be moved to any point along the transmission line where the measurements are desired. Previous measurements [14] have indicated that the time resolution of this technique is about 0.3 ps, and the parasitic loading effect of the external probe is less than 0.1 ps. The frequency-domain attenuation and phase data are obtained from a ratio of the Fourier transforms of any pair of measurement points. Any influence of the needle probe tip is linear and cancels out in the frequency domain, and it is not necessary to explicitly de-embed its response. It is absolutely imperative, however, for the consistency of the data over the THz frequency range that the relative position of the probe and the probing laser beam with respect to the transmission lines remain constant for each measurement point. This is easily achieved through careful measurement techniques.

IV. Discussion of Results

Typical time-domain experimental waveforms are shown in Fig. 4. The launched electrical pulse, measured ~ 200 μm away from the originating gap switch, is ~ 0.6 ps FWHM. This position is taken to be as the origin with length $l = 0.0$ mm. Measurements at various points up to $l = 5.2$ mm are taken. Effects of the finite propagation velocity, attenuation, and dispersion are clearly seen in the pulse propagation data. Qualitatively, we observe the decaying signal amplitude caused by attenuation as well as the broadening of the rising edge and the ringing on the tail of the pulses caused by the frequency dispersion.

Parts (a) and (b) of Fig. 5 show the experimental and the computed effective permittivity ϵ_{eff} for a CPW on GaAs and a CPS on sapphire. The sapphire substrate orientation was unknown and the relative permittivity was taken as the mean of those for the ordinary ($\epsilon_r = 9.4$) and the extraordinary ($\epsilon_r = 11.6$) rays. The fitting parameters were computed from the analytic formulas for a finite

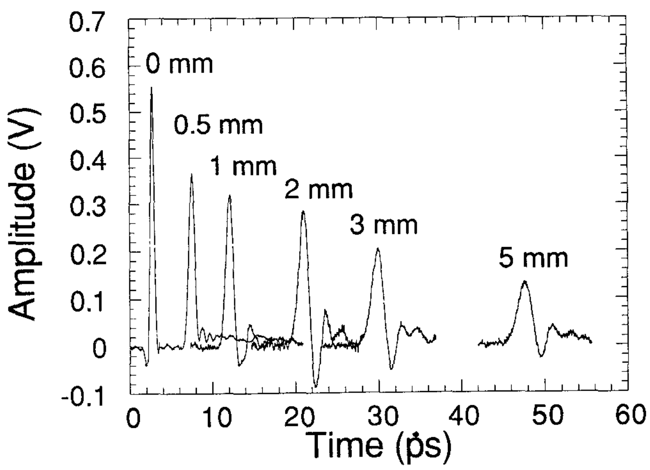

Fig. 4. Typical time-domain picosecond pulse propagation data.

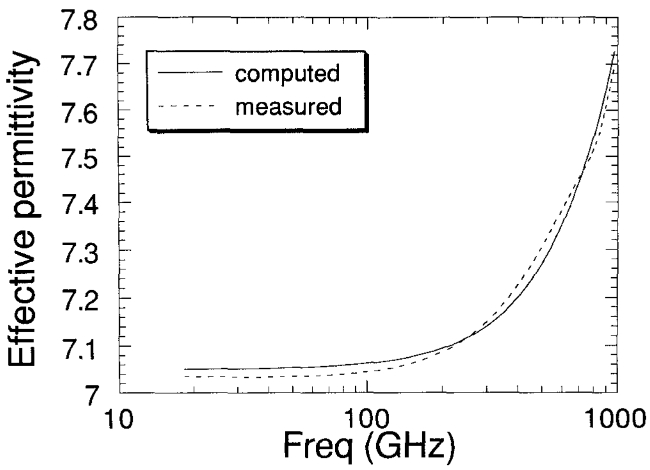

(a)

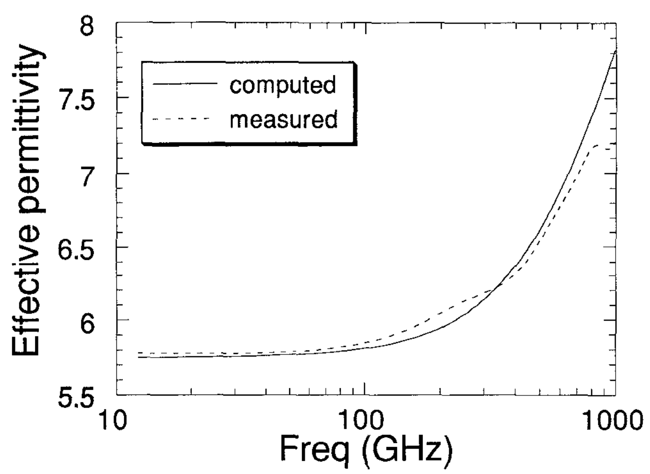

(b)

Fig. 5. Effective permittivity plots. (a) CPW on GaAs measurement and analytic model: $a = 1840$ and $f_{te} = 43$ GHz. (b) CPS on sapphire measurement and analytic model; $a = 193$ and $f_{te} = 57$ GHz.

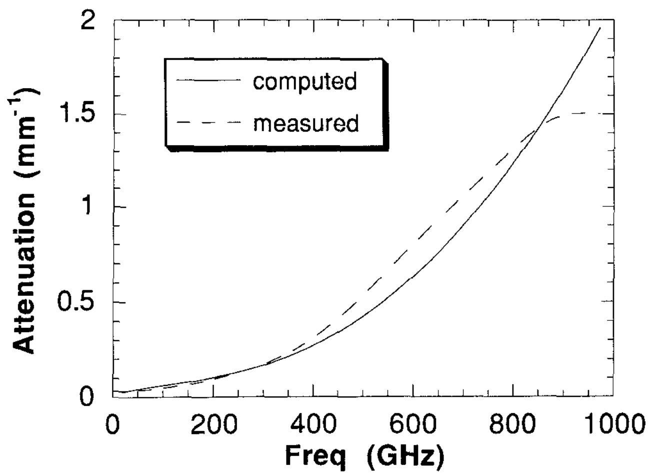

(a)

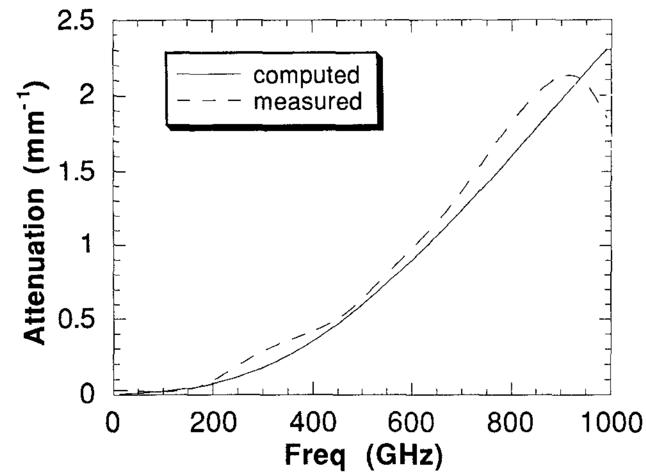

(b)

Fig. 6. Attenuation plots. (a) CPW on GaAs with $a = 1840$ and $f_{te} = 43$ GHz. (b) CPS on sapphire with $a = 193$ and $f_{te} = 57$ GHz.

substrate (eqs. (4a) and (4b)), and their values are shown in the figures for the respective transmission lines.

We can immediately see that there is excellent agreement over the complete THz frequency range. This validates the use of the analytic formulas for the computation of the dispersion behavior of coplanar transmission lines. It also indicates the applicability of the effective permittivity concept.

Parts (a) and (b) of Fig. 6 show the attenuation as a function of frequency from the measurements and the theoretical computations with (8a) and (8b). It is seen that the agreement between the measured and the computed attenuation is very good. The experimental range of accuracy extends to 900 GHz. The rapid roll-off of the measured attenuation near 900 GHz is due to the influence of the spectral noise floor. As the spectral content of the signal measured down the transmission line reaches the noise floor, it appears as an apparent increase in the energy and a roll-off of attenuation at those frequencies.

The good functional agreement for the radiative attenuation between the modified analytic formulas and the

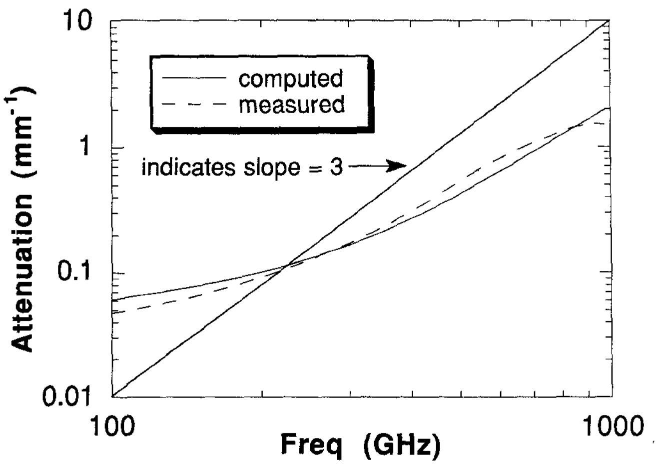

(a)

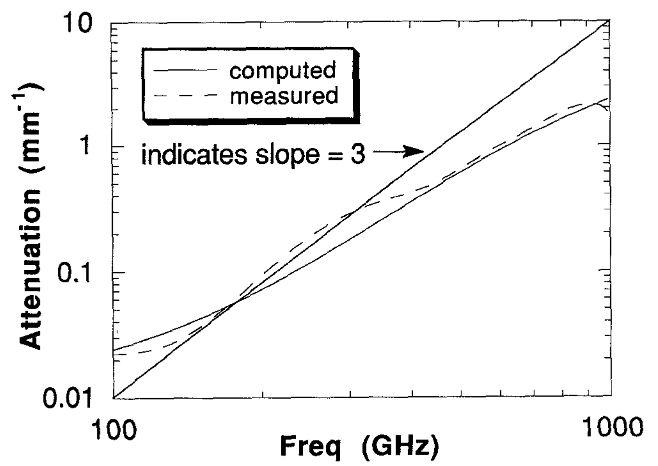

(b)

Fig. 7. Same as Fig. 6 on a log–log scale: (a) CPW; (b) CPS.

measurement can be more clearly seen in parts (a) and (b) of Fig. 7, which are log–log plots. For visualization purposes we have also indicated the slope that would be expected if the losses followed the cubic frequency dependence predicted by the quasi-static approximation to the radiation losses. it is quite apparent that the dependence is closer to a quadratic fit than a cubic one, as is also predicted by the modified formula. The small ripple in the measured attenuation which is visible on the linear plot and is accentuated on the logarithmic one can be shown to be due to a small time-domain waveform truncation error.

V. Conclusion

The tremendous signal bandwidths required by modern electronic technology necessitate coplanar transmission line characterization to THz frequencies. It is also of significant benefit to be able to predict the behavior with a minimum computational effort. We have experimentally verified the analytic dispersion formulas that take into account the transmission line geometry and the substrate thickness for both coplanar waveguide and coplanar striplines. We have also demonstrated the functional inconsistency of the quasi-static radiative loss formula with the measured data at high frequencies. Including the non-quasi-static effects, a roll-off of the radiation loss is predicted. This functional behavior is fully supported by the experimental data over a THz frequency range.

Acknowledgment

The first author would like to acknowledge the many useful discussions and arguments with Prof. G. Rebeiz and J. M. Chwalek and the financial support provided to him by Siemens, Munich. The authors would like to acknowledge the LT-GaAs material growth by F. W. Smith at MIT/LL. The comments and suggestions made by the reviewers are greatly appreciated.

References

[1] A. J. Tessner *et al.*, "Very high performance 0.15 μm gate-length InAlAs/InGaAs/InP lattice matched HEMTs," presented at 12th Biennial IEEE/Cornell University Conf. on Advanced Concepts in High Speed Semiconductor Devices and Circuits.
[2] D. R. Dykaar *et al.*, "High-frequency characterization of thin-film Y-Ba-Cu oxide superconducting transmission lines," *Appl. Phys. Lett.*, vol. 52, no. 17, pp. 1444–1446, Apr. 25, 1988.
[3] M. C. Nuss and K. W. Goosen, "Investigation of high-temperature superconductors with terahertz bandwidth electrical pulses," *IEEE J. Quantum Electron.*, vol. 25, pp. 2596–2607, Dec. 1989.
[4] G. Hasnain, A. Dienes, and J. R. Winnery, "Dispersion of picosecond pulses in coplanar transmission lines," *IEEE Trans. Microwave Theory Tech.*, vol. MTT-34, pp. 738–741, June 1989.
[5] D. Grischkowsky, I. N. Duling III, J. C. Chen, and C.-C. Chi, "Electromagnetic shock waves from transmission lines," *Phys. Rev. Lett.*, vol. 59, no. 15, pp. 1663–1666, Oct. 12, 1987.
[6] D. B. Rutledge, D. P. Neikirk, and D. P. Kasilingham, in *Infrared and Millimeter Waves*, vol. 10, pp. II, K. J. Button, Ed. New York: Academic, 1983.
[7] D. S. Phatak and A. P. Defonzo, "Dispersion characteristics of optically excited coplanar striplines: Pulse propagation," *IEEE Trans. Microwave Theory Tech.*, vol. 38, pp. 654–661, May 1990.
[8] M. Y. Frankel, J. F. Whitaker, G. A. Mourou, J. A. Valdmanis, and P. M. Smith, "100 GHz electrooptic *S*-parameter characterization of high electron mobility transistors," to be presented at Picosecond Electronics and Optoelectronics, Salt Lake City, UT, Mar. 1991.
[9] M. Y. Frankel, R. H. Voelker, G. A. Mourou, R. J. Lomax, unpublished data.
[10] K. C. Gupta, R. Garg, and I. J. Bahl, *Microstrip Lines and Slot Lines*. Norwood, MA: Artech, 1979.
[11] D. H. Auston, A. M. Johnson, P. R. Smith, and J. C. Bean, "Picosecond optoelectronic detection, sampling, and correlation measurements in amorphous semiconductors," *Appl. Phys. Lett.*, vol. 37, pp. 371–373, 1980.
[12] J. A. Valdmanis and R. L. Fork, "Design considerations for a femtosecond pulse laser balancing self phase modulation, group velocity dispersion, saturable absorption and saturable gain," *IEEE J. Quantum Electron.*, vol. QE-22, pp. 112–118, Jan. 1986.
[13] F. W. Smith *et al.*, "Picosecond GaAs-based photoconductive optoelectronic detectors," *Appl. Phys. Lett.*, vol. 54, no. 10, pp. 890–892, Mar. 6, 1989.
[14] J. A. Valdmanis, "1 THz-bandwidth prober for high-speed devices and integrated circuits," *Electron. Lett.*, vol. 23, pp. 1308–1310, 1987.

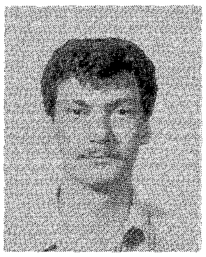

Michael Y. Frankel (S'90) was born in Leningrad, U.S.S.R., in 1964. He received the B.S. degree (magna cum laude) in electrical engineering from the University of Maryland, College Park, in 1986 and the M.S. degree in electrical engineering from the University of Rochester in 1988. He is currently working towards the Ph.D. degree at the Ultrafast Science Laboratory, University of Michigan, Ann Arbor. His interests are in picosecond electronics and optoelectronics, including microwave transmission lines, photodetectors, and transistors. He has applied optoelectronic techniques to high-bandwidth transistor characterization and has developed a large-signal model to analyze transistor power behavior.

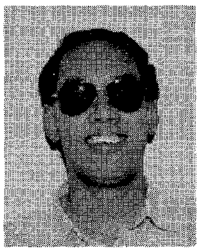

Shantanu Gupta was born in Calcutta, India, in 1965. He received the B. Tech. degree in electrical engineering from the Indian Institute of Technology, Kanpur, India, in 1986, and the M.S. degree in electrical engineering from the University of Rochester, Rochester, NY, in 1988. Since then, he has been working towards the Ph.D. degree in electrical engineering at the University of Michigan, Ann Arbor. He has worked on the generation, detection, and application of subpicosecond electrical pulses in III–V semiconductors. Currently he is studying ultrafast phenomena in III–V semiconductors using femtosecond laser techniques. His research also includes the study of femtosecond optical interactions in fibers in the 1.5 μm wavelength region.

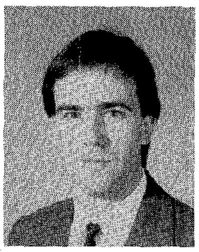

Janis A. Valdmanis was born in Old Windsor, England, in 1956 and emigrated to the United States in 1967. He received the B.S. degrees in physics and mathematics from Purdue University, West Lafayette, IN, in 1978 and the Ph.D. degree in optics from the University of Rochester's Institute of Optics, Rochester, NY, in association with the University's Laboratory for Laser Energetics in 1983.

From 1983 to 1988, he was a member of technical staff at AT&T Bell Laboratories, Murray Hill, NJ. In September of 1988, he moved to the University of Michigan in Ann Arbor as an Associate Professor of Optics in the Electrical Engineering and Computer Science Department. He is also the associate director of the Ultrafast Science Laboratory. His current research interests are focused on femtosecond laser systems and ultrafast optoelectronic instrumentation.

Dr. Valdmanis is a Fellow of the Optical Society of America (1990), and in 1988 he received the Society's Adolph Lomb Medal for his contributions to ultrafast optical instrumentation.

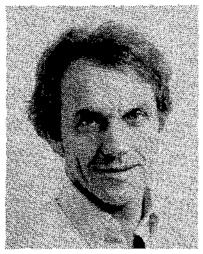

Gerard A. Mourou (M'89) is Director of the Ultrafast Science Laboratory (USL), formed in 1988 within the Department of Electrical Engineering and Computer Science at the University of Michigan. USL is now the largest laboratory working in the field of ultrafast science in the nation. He also holds a joint appointment in the Deparment of Electrical Engineering and the Department of Applied Physics. Under his direct supervision is a research group of 30 scientists and engineers, nearly half are Ph.D. students.

He received the Ph.D. degree in physics from the University of Paris. From 1978 to September 1988 Dr. Mourou was a scientist at the University of Rochester Laboratory for Laser Energetics (LLE). At the University of Rochester he held joint appointments as a professor at the Institute of Optics and as the Director for Ultrafast Science and Technology at LLE. He is a scientific advisor to the French Atomic Energy Commission and a consultant to several private and governmental organizations, including the Lawrence Livermore National Laboratory, Xerox Corporation, Hypres Inc., INRAD, and Medox, Inc. He also serves on the Scientific Board of the Laboratory for Optics of the Ecole Polytechnique—ENSTA and on the Editorial Board of *Laser Focus*. Dr. Mourou was the initiator and cochair of the Picosecond Electronics and Optoelectronics Conference, the first conference to bridge the fields of ultrafast optics and electronics; he is chair of the Ultrafast Phenomena Conference.

Dr. Mourou has been a pioneer in the field of ultrafast photonics for nearly 20 years. He has published more than 100 scientific papers and holds nine patents and six patent applications on ultrafast laser techniques and applications. He is the coinventor of the electro-optic sampling technique that is considered the best way to characterize ultrafast transistors and circuits. He is also the coinventor of the laser technique known as chirped pulse amplification, which allows the generation of ultrahigh peak-power pulses. His leisure activities include squash, downhill skiing, and classical music.